

Supplementary Materials

Di- and Trinuclear Sandwich Complexes of a Cross-conjugated Fulvene

Eiji Kudo, Yuki Oba, Koji Yamamoto, and Tetsuro Murahashi

*Department of Chemical Science and Engineering,
School of Materials and Chemical Technology, Tokyo Institute of Technology,
O-okayama, Meguro-ku, Tokyo 152-8552, Japan.*

Table of Contents

Experimental Section	S3-14
<i>General Consideration</i>	S3
<i>Synthesis of [Pd₂(6,6-dimethylfulvene)₂(CH₃CN)₂]₂[BF₄]₂ (2a)</i>	S3
<i>Synthesis of [Pd₂(6,6-diphenylfulvene)₂(CH₃CN)₂]₂[BF₄]₂ (2b)</i>	S6
<i>Synthesis of Pd₂(6,6-diphenylfulvene)₂Cl₂ (2b-Cl)</i>	S9
<i>Synthesis of [Pd₃(6,6-dimethylfulvene)₂(CH₃CN)₃]₂[BF₄]₂ (3a)</i>	S12
<i>Synthesis of [Pd₃(6,6-diphenylfulvene)₂(CH₃CN)₂]₂[BF₄]₂ (3b)</i>	S15
<i>Synthesis of [Pd₂(CH₃CN)₂(μ-6,6-diphenylfulvene) (μ₃-6,6-diphenylfulvene)Pd(CH₃CN)₂]₂[BF₄]₂ (4)</i>	S18
Computational Details	S21-31
X-ray Crystallographic analyses	S32-39
References	S40-41

Experimental Section

General Consideration. All manipulations were conducted under a nitrogen atmosphere using standard Schlenk or dry-box technique. ^1H and $^{13}\text{C}\{^1\text{H}\}$ NMR spectra were recorded on 400 MHz instruments (JEOL JNM-ECZ400S). The chemical shifts were referenced to the residual resonances of deuterated solvents. Elemental analyses were performed on a PerkinElmer 2400II series CHN analyzer. X-ray crystal data were collected by Rigaku RAXIS-RAPID imaging plate diffractometer. ESI-MS spectra were recorded on Bruker micrOTOF ESI-TOF. Unless specified, all reagents were purchased from commercial suppliers and used without purification. CH_2Cl_2 , CH_3NO_2 , CH_3CN , benzene, toluene, *n*-hexane, diethyl ether, CD_3NO_2 , and CDCl_3 , were purified according to the standard procedures. $[\text{Pd}_2(\text{CH}_3\text{CN})_6][\text{BF}_4]_2$ (**1**)^[S1] and $\text{Pd}_2(\text{dba})_3 \cdot \text{CHCl}_3$ ^[S2] were prepared according to the literature.

Synthesis of $[\text{Pd}_2(6,6\text{-dimethylfulvene})_2(\text{CH}_3\text{CN})_2][\text{BF}_4]_2$ (2a**):** $[\text{Pd}_2(\text{CH}_3\text{CN})_6][\text{BF}_4]_2$ (264.8 mg, 4.18×10^{-1} mmol) and 6,6-dimethylfulvene (97.8 mg, 9.21×10^{-1} mmol) were dissolved in CH_3NO_2 under N_2 atmosphere. After stirring for 10 min, the reaction mixture was filtered through Celite, and the Celite was washed with dichloromethane. The solution was concentrated, and precipitated with toluene. The solid was washed with toluene and Et_2O , and dried under reduced pressure to give complex **2a** as an orange solid (230.6 mg, 3.39×10^{-1} mmol, 81% yield). ^1H NMR (400 MHz, CD_3NO_2 , 25 °C): δ 7.10 (br, 4H, H_1), 6.43 (br, 4H, H_2), 2.48 (br, 4H, CH_3CN), 2.29 (s, 12H, H_5). $^{13}\text{C}\{^1\text{H}\}$ NMR (101 MHz): δ 169.2 (C_4), 139.8 (C_3), 126.2 (CH_3CN), 102.3 (C_2), 94.3 (C_1), 25.1 (C_5), 3.2 (CH_3CN). HRMS-EI (m/z): $[\text{M}]^+$ calcd for $\text{C}_{20}\text{H}_{26}\text{N}_2\text{Pd}_2$, 254.0084; found, 254.0129.

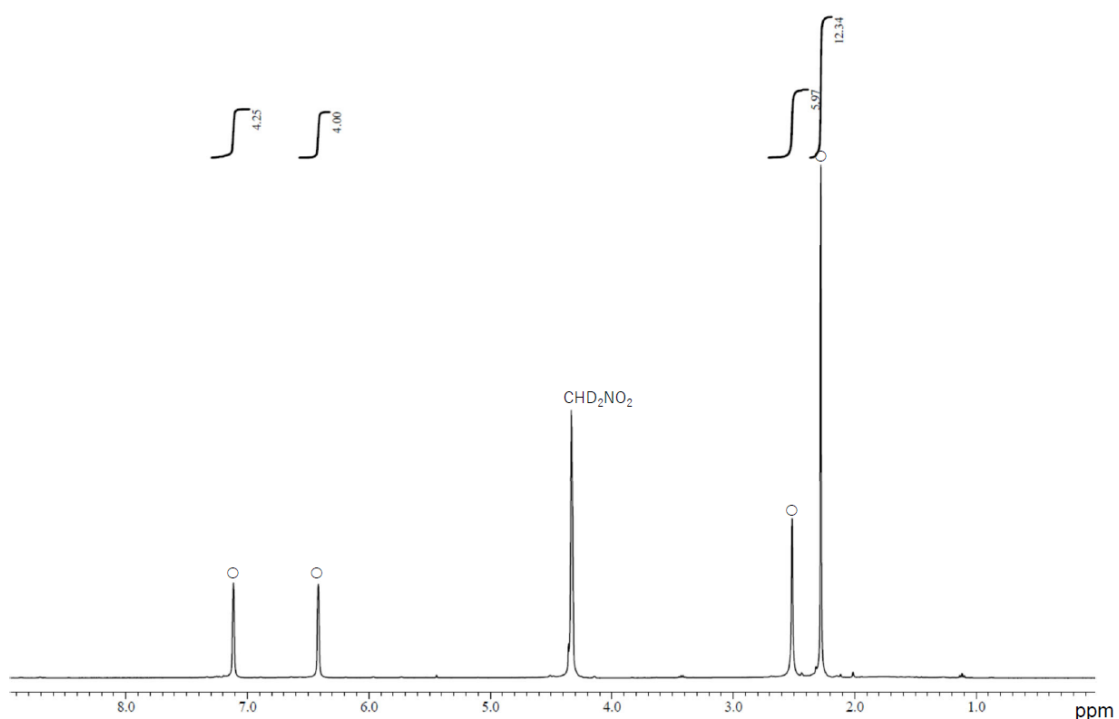
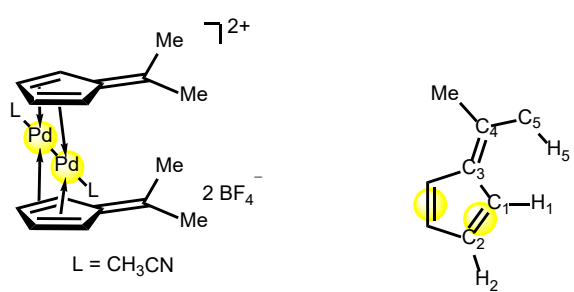


Figure S1. ^1H NMR spectrum of complex **2a**. ○ = $[\text{Pd}_2(6,6\text{-dimethylfulvene})_2(\text{CH}_3\text{CN})_2][\text{BF}_4]_2$.

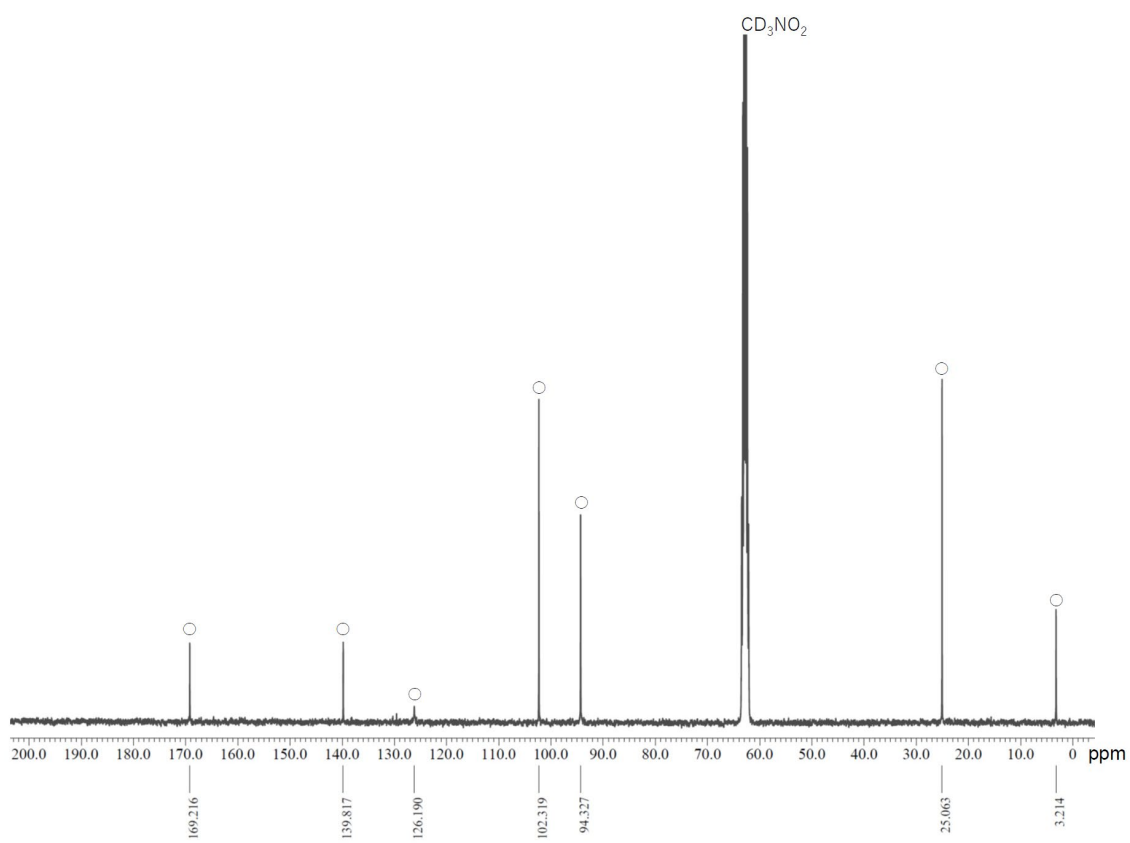
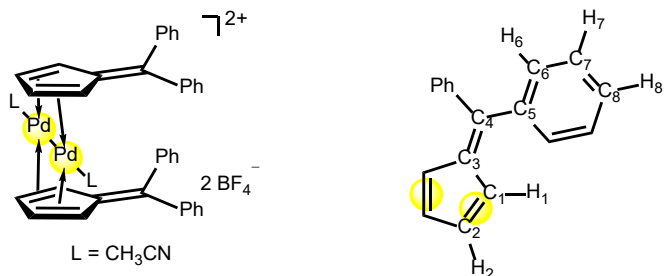


Figure S2. ¹³C NMR spectrum of complex **2a**. ○ = $[\text{Pd}_2(6,6\text{-dimethylfulvene})_2(\text{CH}_3\text{CN})_2][\text{BF}_4]_2$.

Synthesis of $[\text{Pd}_2(6,6\text{-diphenylfulvene})_2(\text{CH}_3\text{CN})_2][\text{BF}_4]_2$ (2b**):** $[\text{Pd}_2(\text{CH}_3\text{CN})_6][\text{BF}_4]_2$ (50 mg, 7.9×10^{-2} mmol) and 6,6-diphenylfulvene (36.0 mg, 1.56×10^{-1} mmol) were dissolved in CH_3NO_2 and stirred for 10 min at room temperature. The reaction mixture was diluted by CH_2Cl_2 , and then filtered. Addition of toluene to the solution afforded red microcrystal of complex **2b** (47.3 mg, 5.09×10^{-2} mmol, 64% yield). The single crystal of **2b** was obtained by recrystallization from benzene/ CH_3NO_2 at room temperature. ^1H NMR (400 MHz, CD_3NO_2 , 25 °C): δ 7.69, (t, $J = 7.6$ Hz, 4H, H₈), 7.46 (dd, $J = 7.6, 7.6$ Hz, 8H, H₇), 7.35 (d, $J = 7.6$ Hz, 8H, H₆), 6.96-6.94 (m, 4H, H₁), 6.65-6.63 (m, 4H, H₂), 2.27 (s, 6H, CH_3CN). $^{13}\text{C}\{\text{H}\}$ NMR (101 MHz) δ 162.6 (C₄), 140.7 (C₅), 139.5 (C₃), 134.0 (C₆), 133.4 (C₈), 130.2 (C₇), 125.4 (CH_3CN), 102.3 (C₂), 97.6 (C₁), 2.9 (CH_3CN). Anal. Calcd. for $\text{C}_{40}\text{H}_{36}\text{B}_2\text{F}_8\text{N}_2\text{OPd}_3$: C, 50.72; H, 3.83 N, 2.96. Found: C, 50.64; H, 3.73 N, 2.84.



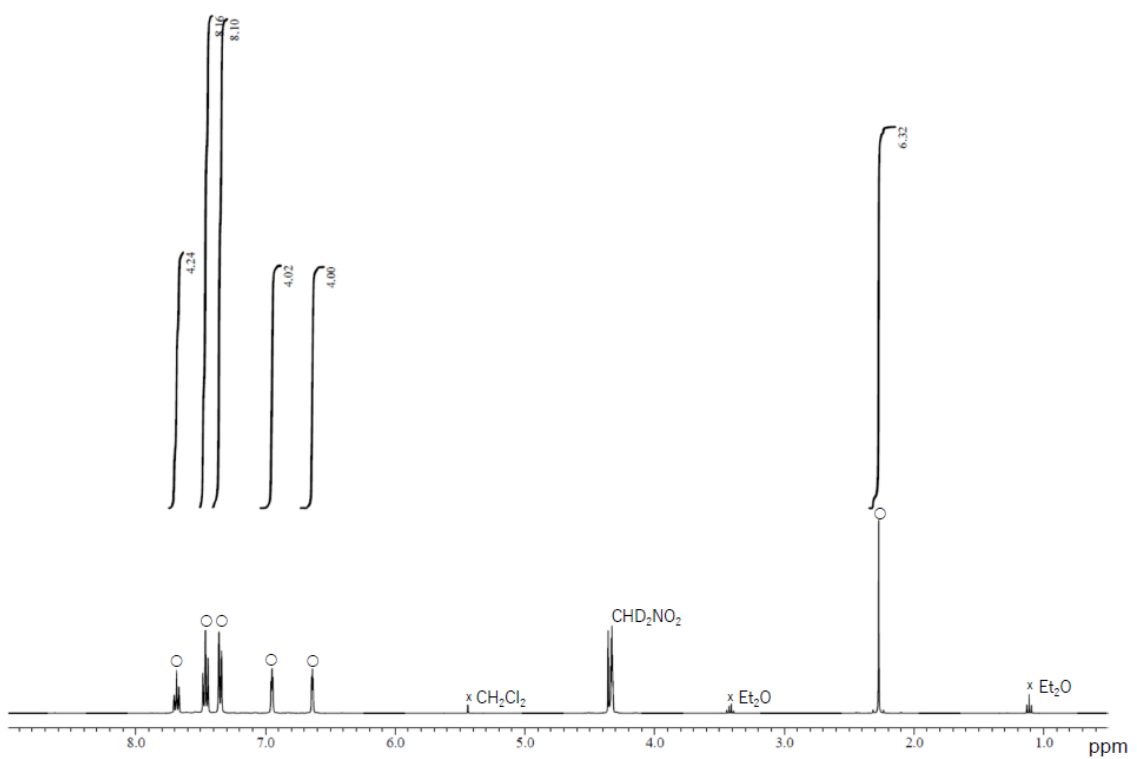


Figure S3. ¹H NMR spectrum of complex **2b**. ○ = [Pd₂(6,6-diphenylfulvene)₂(CH₃CN)₂][BF₄]₂, x = impurities.

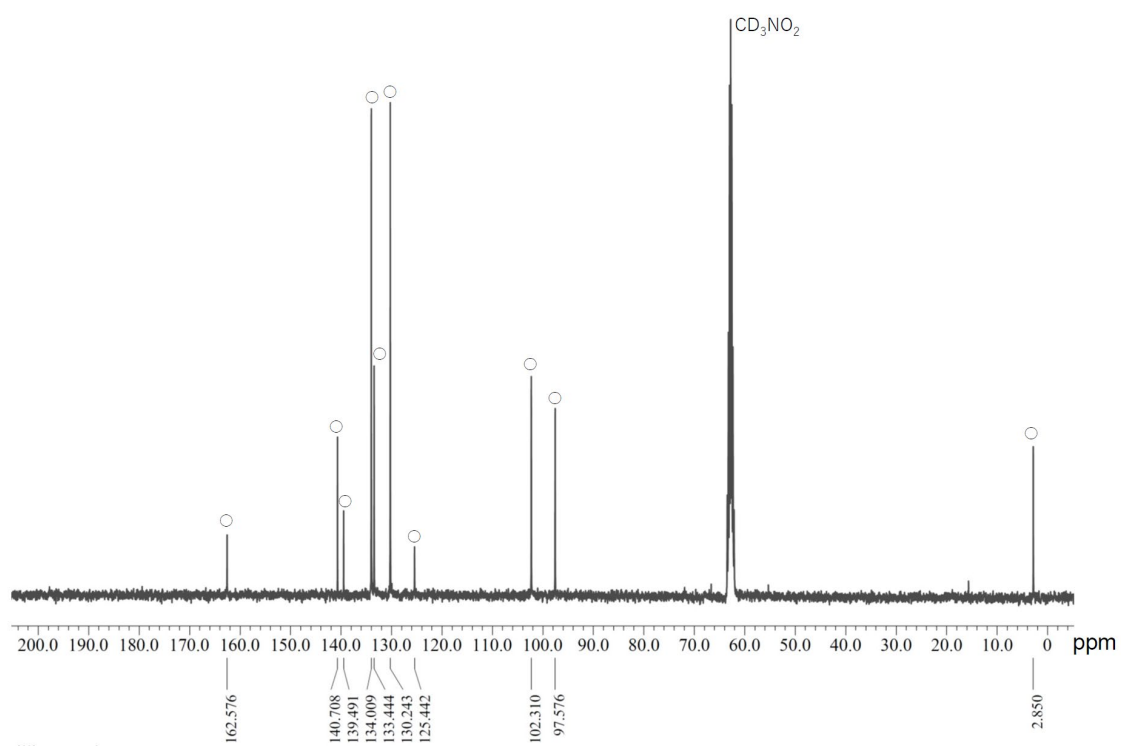
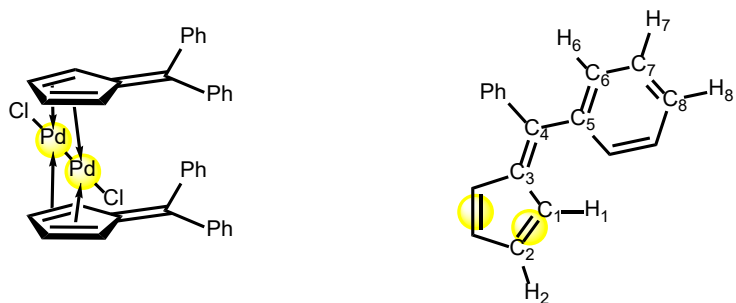


Figure S4. ^{13}C NMR spectrum of complex **2b**. ○ = $[\text{Pd}_2(6,6\text{-diphenylfulvene})_2(\text{CH}_3\text{CN})_2][\text{BF}_4]_2$.

Synthesis of Pd₂(6,6-diphenylfulvene)₂Cl₂ (2b-Cl): [Pd₂(CH₃CN)₆][BF₄]₂ (100 mg, 1.58 x 10⁻¹ mmol) and 6,6-diphenylfulvene (72.0 mg, 3.13 x 10⁻¹ mmol) were dissolved in CHCl₃/CH₃NO₂ and stirred for 10 min at room temperature. Following procedures were conducted under air. Brine (5 mL) was added to the solution, and then the reaction mixture was stirred for 5 min. The reaction mixture was extracted by CHCl₃. The combined organic layers were dried over Na₂SO₄ and filtered. The solvent was concentrated under reduced pressure to give complex **2b-Cl** (110.3 mg, 1.48 x 10⁻¹ mmol, 94 % yield) as a red solid. The single crystal suitable for X-ray diffraction analysis was obtained by recrystallization from cyclohexane/CH₂Cl₂ at room temperature. ¹H NMR (400 MHz, CDCl₃, 25 °C) δ 7.54-7.40 (m, 4H, H₈), 7.37-7.21 (m, 16H, H₆ and H₇), 6.93-6.87 (m, 4H, H₁), 6.14-6.08 (m, 4H, H₂). ¹³C{¹H} NMR (101 MHz) δ 156.1 (C₄), 139.7 (C₅), 137.7 (C₃), 132.2 (C₆ or C₇), 130.8 (C₈), 129.6 (C₆ or C₇), 95.9 (C₂), 94.7 (C₁). Anal. Calcd. for C₃₆H₂₈Cl₂Pd₂·H₂O: C, 56.72; H, 3.97. Found: C, 56.53; H, 4.36.



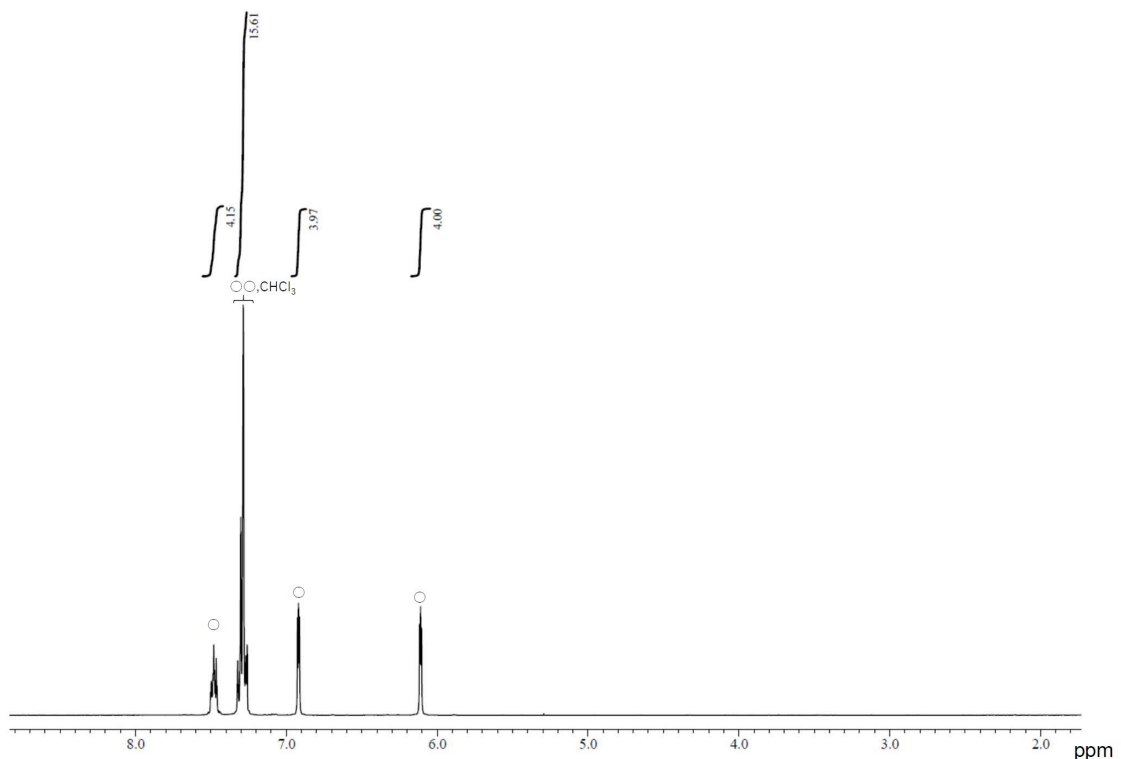


Figure S5. ^1H NMR spectrum of complex **2b-Cl**. $\circ = \text{Pd}_2(6,6\text{-diphenylfulvene})_2\text{Cl}_2$.

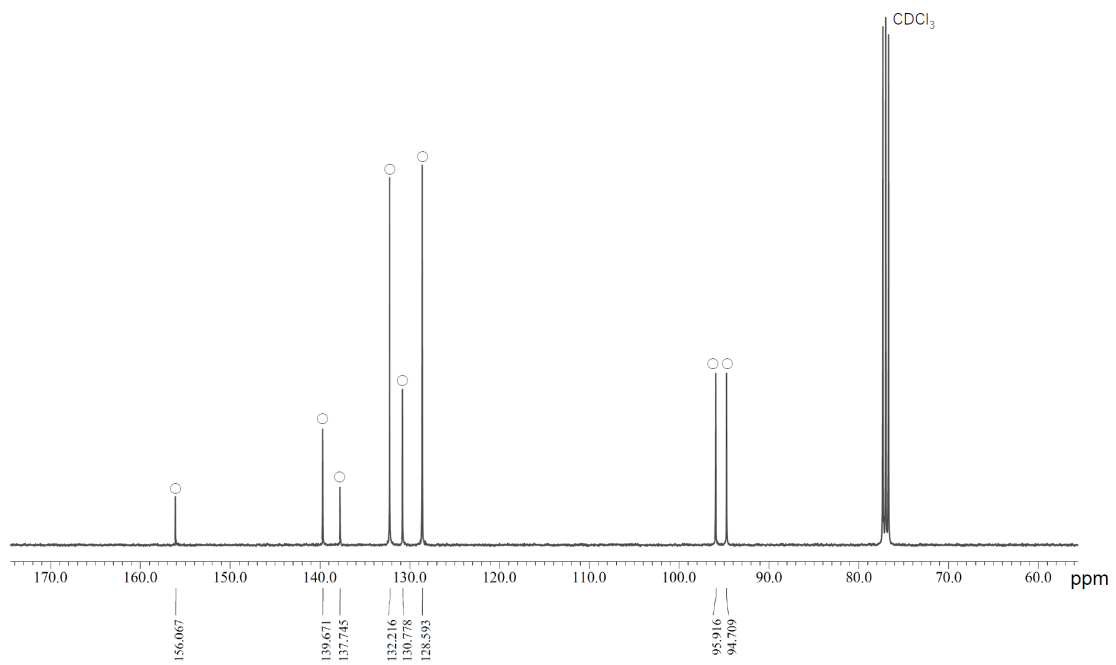
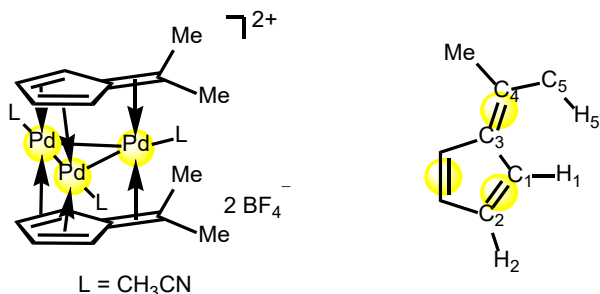


Figure S6. ^{13}C NMR spectrum of complex **2b-Cl**. $\circ = \text{Pd}_2(6,6\text{-diphenylfulvene})_2\text{Cl}_2$.

Synthesis of $[Pd_3(6,6\text{-dimethylfulvene})_2(CH_3CN)_3][BF_4]_2$ (3a): To a nitromethane solution of complex **2a** (300.8 mg, 4.42×10^{-1} mmol) was added $Pd_2(dbu)_3 \cdot CHCl_3$ (237.9 mg, 2.30×10^{-1} mmol) and acetonitrile (50 μL , 9.57×10^{-1} mmol) in dichloromethane under N_2 atmosphere . After stirring overnight, the reaction mixture was filtered through Celite, and the Celite was washed with dichloromethane. The solution was concentrated, and precipitated with toluene. The solid was washed with toluene and Et_2O , and dried under reduced pressure to give complex **3a** as a brown solid (294.3 mg, 3.55×10^{-1} mmol, 80% yield). 1H NMR (400 MHz, CD_3NO_2 , 25 °C): δ 5.95 (br, 4H, H_2), 5.73 (br, 4H, H_1), 2.41 (br, 6H, CH_3CN), 2.01 (s, 12H, H_5). $^{13}C\{^1H\}$ NMR (101 MHz): δ 109.0 (C_3), 99.2 (C_4), 89.8 (C_2), 83.7 (C_1), 24.0 (C_5), 3.0 (CH_3CN). HRMS-EI (m/z): $[M]^+$ calcd for $C_{22}H_{29}N_3Pd_3$, 327.4736; found, 327.4797.



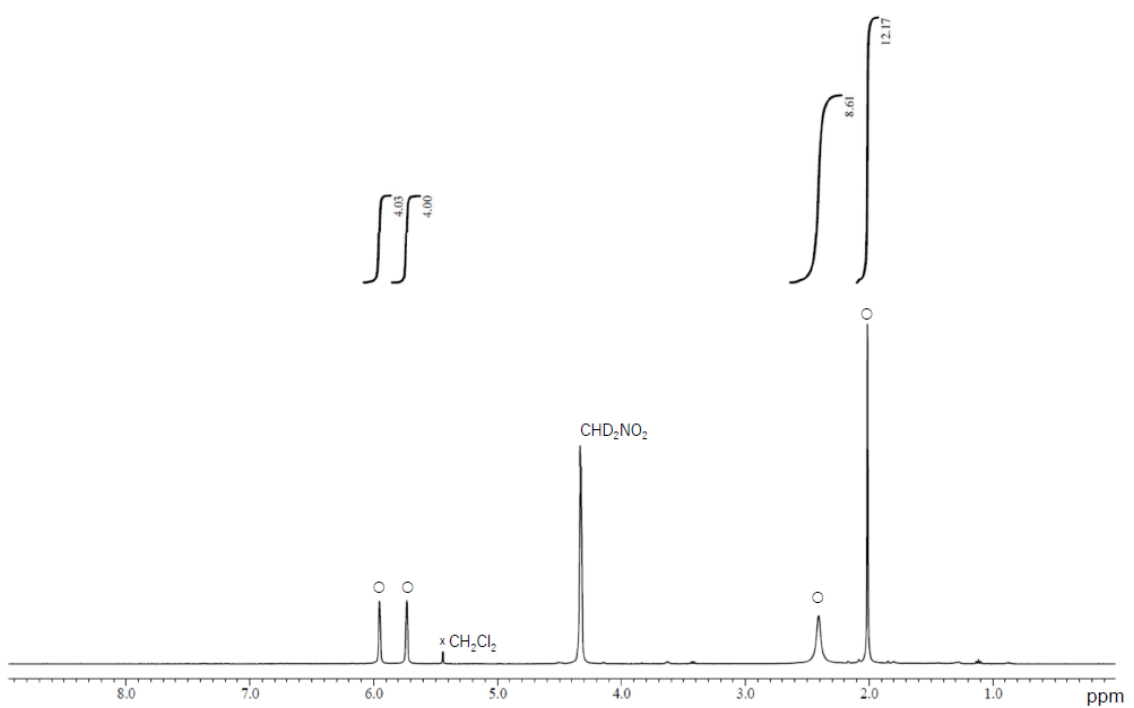


Figure S7. ^1H NMR spectrum of complex **3a**. ○ = $[\text{Pd}_3(6,6\text{-dimethylfulvene})_2(\text{CH}_3\text{CN})_3][\text{BF}_4]_2$.

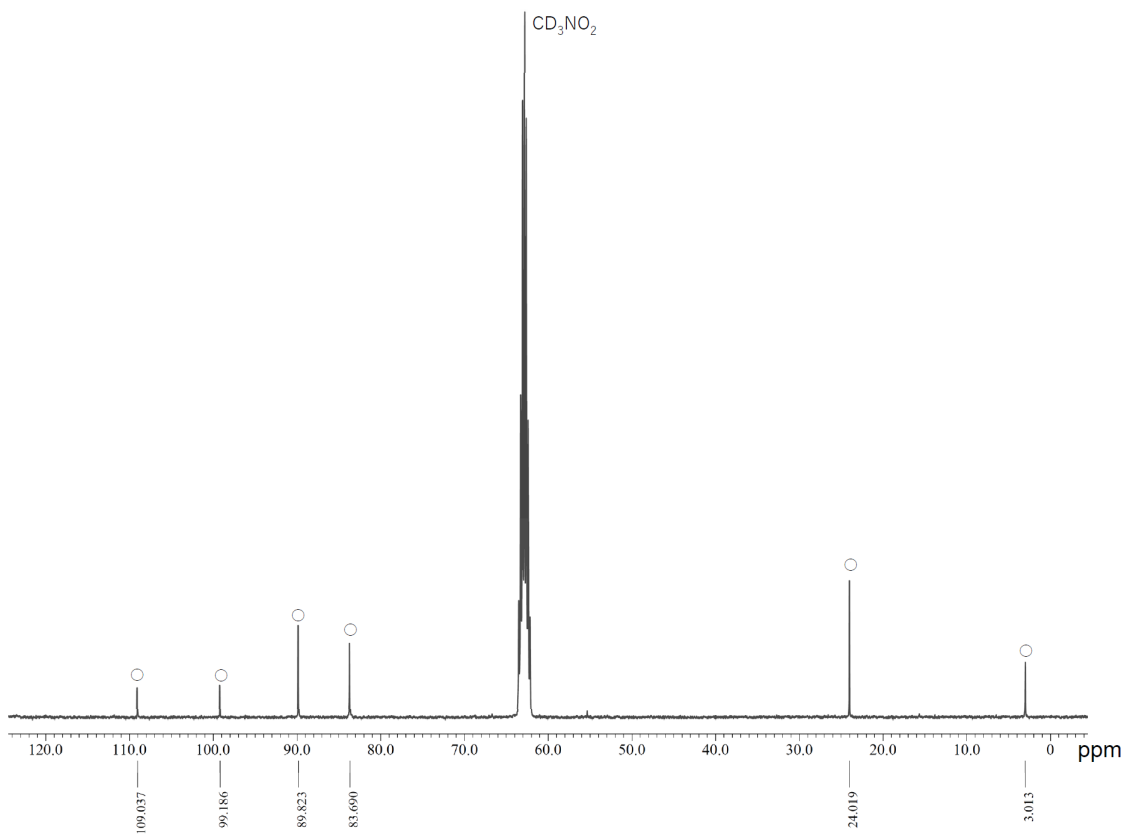
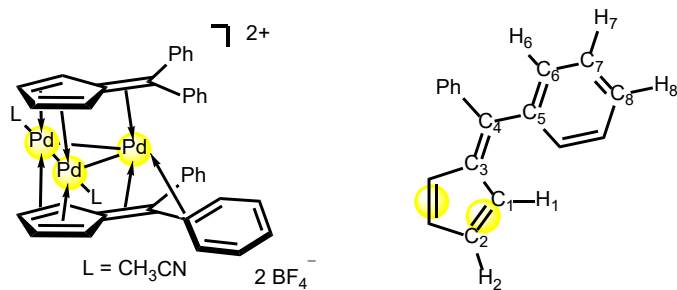


Figure S8. ^{13}C NMR spectrum of complex **3a**. ○ = $[\text{Pd}_3(6,6\text{-dimethylfulvene})_2(\text{CH}_3\text{CN})_3][\text{BF}_4]_2$.

Synthesis of $[Pd_3(6,6\text{-diphenylfulvene})_2(CH_3CN)_2][BF_4]_2$ (3b**):** $[Pd_2(CH_3CN)_6][BF_4]_2$ (100 mg, 1.58×10^{-1} mmol) and 6,6-diphenylfulvene (72.0 mg, 3.13×10^{-1} mmol) were dissolved in CH_2Cl_2/CH_3NO_2 under N_2 atmosphere . After stirring for 10 min, $Pd_2(dba)_3 \cdot CHCl_3$ (86.7 mg, 8.38×10^{-2} mmol) was added to the reaction mixture, and then the reaction mixture was stirred for 4 h at room temperature. The reaction mixture was filtered. Addition of Et_2O to the solution afforded precipitate. The solid was washed with Et_2O several times and dried under reduced pressure to give complex **3b** as a red solid (113.6 mg, 1.10×10^{-1} mmol, 69% yield). The single crystal suitable for X-ray diffraction analysis was obtained by recrystallization from toluene/ CH_3NO_2, CH_2Cl_2 at -20 °C. 1H NMR (400 MHz, CD_3NO_2 , 25 °C): δ 7.52-7.39 (m, 12H, H_7 and H_8), 7.16 (d, $J = 7.6$ Hz, 8H, H_6), 6.35-6.28 (m, 4H, H_2), 6.01-5.96 (m, 4H, H_1), 2.28 (s, CH_3CN , 6H). $^{13}C\{^1H\}$ NMR (101 MHz) δ 135.7 (C_5), 134.0 (C_4), 132.8 (C_8), 131.1 (C_7), 130.4 (C_6), 125.1 (CH_3CN), 108.5 (C_3), 90.8 (C_2), 88.7 (C_1), 2.9 (CH_3CN). Anal. Calcd. for $C_{40}H_{34}B_2F_8N_2Pd_3$: C, 46.39; H, 3.31 N, 2.71. Found: C, 46.45; H, 3.31 N, 2.84.



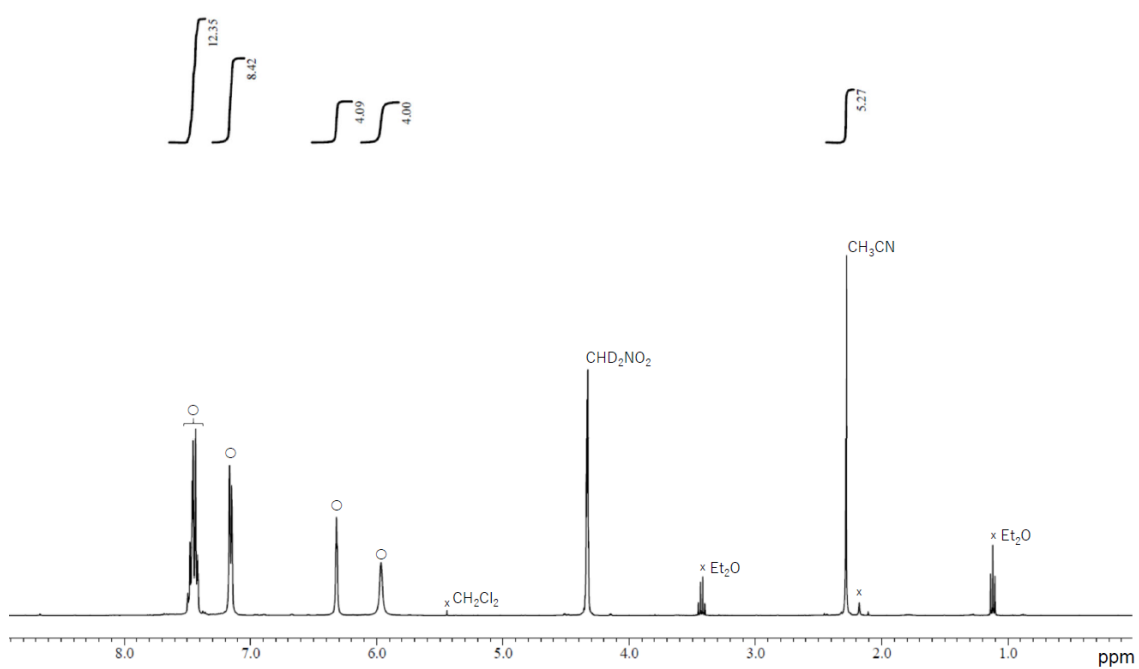


Figure S9. ^1H NMR spectrum of complex **3b**. ○ = $[\text{Pd}_3(6,6\text{-diphenylfulvene})_2(\text{CH}_3\text{CN})_2][\text{BF}_4]_2$, x = impurities.

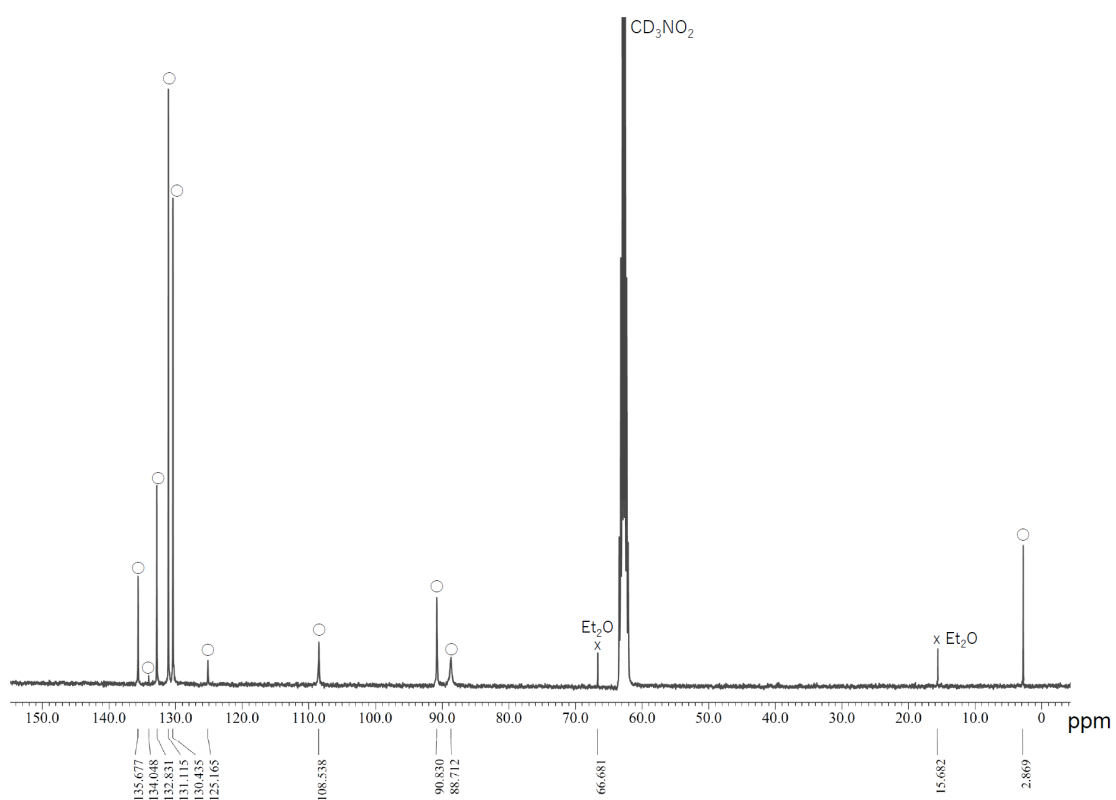
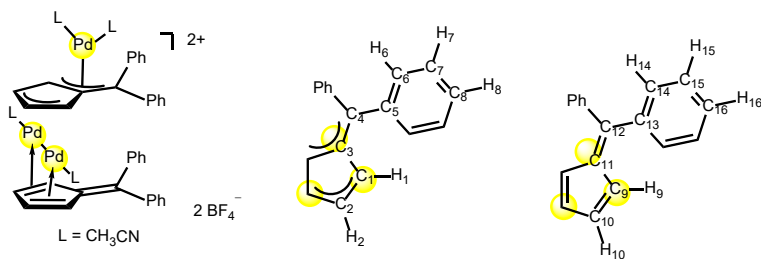


Figure S10. ^{13}C NMR spectrum of complex **3b**. ○ = $[\text{Pd}_3(6,6\text{-diphenylfulvene})_2(\text{CH}_3\text{CN})_2][\text{BF}_4]_2$, x = impurities.

Synthesis of $[\text{Pd}_2(\text{CH}_3\text{CN})_2(\mu\text{-}\eta^2\text{:}\eta^2\text{-6,6-diphenylfulvene})(\mu_3\text{-}\eta^1\text{:}\eta^2\text{:}\eta^3\text{-6,6-diphenylfulvene})\text{Pd}(\text{CH}_3\text{CN})_2][\text{BF}_4]_2$ (4): Complex **3b** was quantitatively converted to $[\text{Pd}_2(\text{CH}_3\text{CN})_2(\mu\text{-6,6-diphenylfulvene})(\mu_3\text{-6,6-diphenylfulvene})\text{Pd}(\text{CH}_3\text{CN})_2][\text{BF}_4]_2$ (**4**) in CD_3CN . The single crystal suitable for X-ray diffraction analysis was obtained by recrystallization from toluene/ CH_3CN at -20 °C. ^1H NMR (400 MHz, CD_3CN , 25 °C): δ 7.56 (t, $J = 7.2$ Hz, 2H, H_8), 7.16 (dd, $J = 7.2, 7.2$ Hz, 4H, H_7), 7.40 (d, $J = 7.2$ Hz, 4H, H_6), 7.33 (brt, $J = 8.0$ Hz, 2H, H_{16}), 7.16 (d, $J = 7.2$ Hz, 4H, H_{14}), 7.08 (dd, $J = 7.2, 8.0$ Hz, 4H, H_{15}), 6.07-6.02 (m, 2H, H_9), 6.02-5.97 (m, 2H, H_{10}), 5.92-5.85 (m, 2H, H_2), 5.37-5.27 (m, 2H, H_1). $^{13}\text{C}\{\text{H}\}$ NMR (101 MHz): δ 151.3 (C_{12}), 142.1 (C_{11}), 141.8 (C_5), 141.2 (C_{13}), 131.8, 131.0, 131.0, 129.6, 129.5, 129.5 (C_{6-8} and C_{14-16}), 121.9 (C_3), 95.6 (C_9), 94.5(C_{10}), 89.3 (C_2), 86.0, (C_4), 70.1 (C_1). HRMS-EI (m/z): [M] $^{2+}$ calcd for $\text{C}_{44}\text{H}_{40}\text{N}_4\text{Pd}_3$, 472.0186; found, 472.0193.



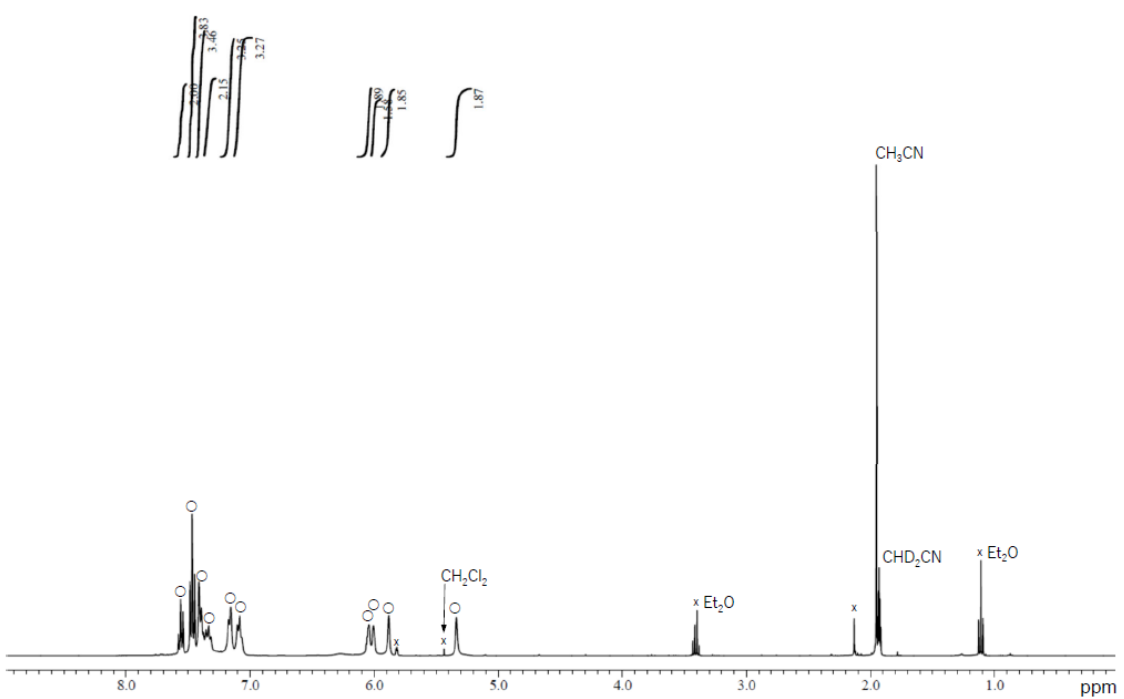


Figure S11. ^1H NMR spectrum of complex **4**. ○ = $[\text{Pd}_2(\text{CH}_3\text{CN})_2(\mu\text{-}6,6\text{-diphenylfulvene})(\mu_3\text{-}6,6\text{-diphenylfulvene})\text{Pd}(\text{CH}_3\text{CN})_2][\text{BF}_4]_2$, x = impurities.

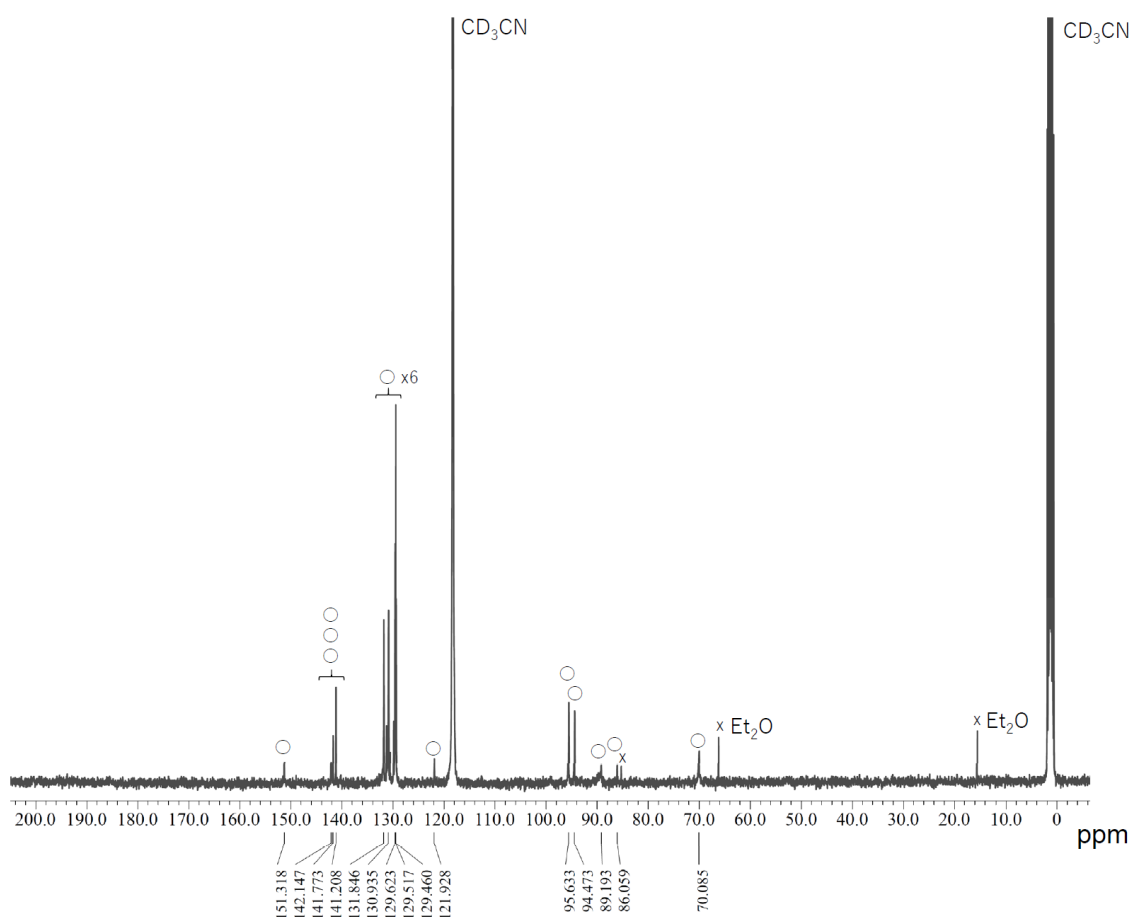


Figure S12. ^{13}C NMR spectrum of complex **4**. ○ = $[\text{Pd}_2(\text{CH}_3\text{CN})_2(\mu\text{-}6,6\text{-diphenylfulvene})(\mu_3\text{-}6,6\text{-diphenylfulvene})\text{Pd}(\text{CH}_3\text{CN})_2][\text{BF}_4]_2$, x = impurities.

Computational Details: All calculations were carried out with Gaussian09 program package (Revision D.01).^[S3] Geometrical optimization was performed with DFT method using the M06 functional.^[S4] Core electrons of Pd were replaced with Stuttgart-Dresden-Bonn relativistic effect core potentials (ECPs) and their valence electrons were represented by (8s7p6d)/[6s5p3d] basis set.^[S5] Usual 6-311G(d) basis sets were used for other atoms.^[S6] The optimized structures of $[\text{Pd}_3(\mu_3\text{-dimethylfulvene})_2(\text{HCN})_2]^{2+}$ (**2a'**), $[\text{Pd}_3(\mu_3\text{-dimethylfulvene})_2(\text{HCN})_3]^{2+}$ (**3a'**), and fulvene were depicted in Figures S13, S16, and S19, respectively. Cartesian coordinates of the optimized geometries of **2a'**, **3a'** and 6,6-dimethylfulvene were shown in Tables S1-S3. The selected molecular orbitals of **2a'**, **3a'** and 6,6-dimethylfulvene were shown in Figures S14, S17, and S20, respectively. Natural atomic orbital (NAO) population analyses were performed with NBO analysis version 3.1.^[S7] A summary of NAO population for each atom in **2a'**, **3a'** and 6,6-dimethylfulvene was shown in Figures S15, S18, and S21, respectively. Mayer bond indices (MBIs) were evaluated by the program BORDER.^[S8] A summary of selected bond lengths, MBIs, and NAO population analysis was shown in Figure S22.

Table S1. Cartesian coordinates (in Å) of the optimized geometry of $[\text{Pd}_2(\mu\text{-dimethylfulvene})_2(\text{HCN})_2]^{2+}$ (**2a'**).

Symbol	X	Y	Z
Pd	-1.2846876	0.0014480	-0.6445242
N	-3.4329541	0.0039352	-0.6232186
C	-1.1629849	2.2158643	-0.2641202
H	-2.1774942	2.4801186	0.0135562
C	-0.7177984	2.0722553	-1.5820655
H	-1.3342790	2.1195424	-2.4735437
C	0.7230310	2.0706822	-1.5819440
H	1.3397741	2.1165009	-2.4733169
C	1.1683179	2.2133698	-0.2639384
H	2.1833703	2.4753671	0.0138872
C	0.0027381	2.3436485	0.6091023
C	0.0028844	2.6010929	1.9511864
C	-1.2479939	2.7759058	2.7291545
H	-1.2999219	3.8017916	3.1186075
H	-1.2395831	2.1307278	3.6163517
H	-2.1625285	2.5798457	2.1682166
C	1.2539326	2.7732318	2.7294524
H	1.2451687	2.1256782	3.6149402
H	1.3065022	3.7980031	3.1216998
H	2.1683203	2.5780648	2.1679805
C	-4.5755517	0.0053548	-0.6857874
Pd	1.2851351	-0.0013994	-0.6438567
N	3.4334040	-0.0039841	-0.6218333
C	1.1632634	-2.2158661	-0.2632655
H	2.1775740	-2.4800097	0.0152404
C	0.7191450	-2.0721773	-1.5815644
H	1.3363309	-2.1194815	-2.4725550
C	-0.7216860	-2.0705617	-1.5825818
H	-1.3377199	-2.1162972	-2.4744484
C	-1.1680389	-2.2132971	-0.2649421
H	-2.1832860	-2.4754391	0.0120307
C	-0.0031358	-2.3436682	0.6090194
C	-0.0043582	-2.6012106	1.9510848
C	1.2458644	-2.7761725	2.7300672
H	1.2971425	-3.8019369	3.1199185
H	1.2369820	-2.1306867	3.6170399
H	2.1609010	-2.5806121	2.1697801
C	-1.2560602	-2.7732426	2.7283290
H	-1.2476966	-2.1261970	3.6141871
H	-1.3093532	-3.7982170	3.1199553
H	-2.1699422	-2.5773799	2.1662712
C	4.5760179	-0.0054085	-0.6841286

H	-5.6498998	0.0067130	-0.7475817
H	5.6503813	-0.0067905	-0.7456804

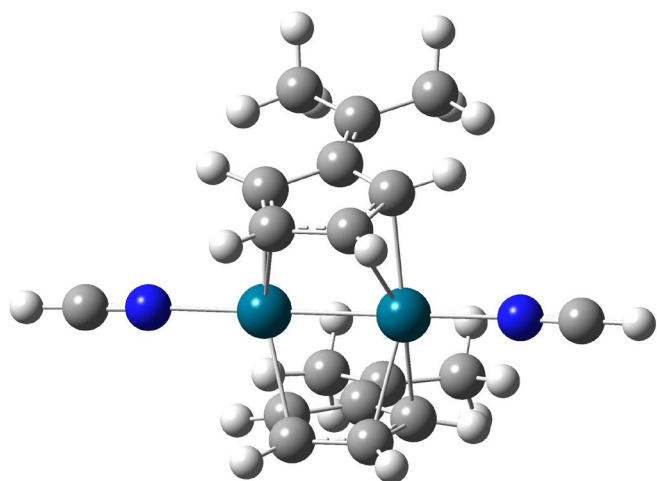


Figure S13. The optimized geometry of $[\text{Pd}(\mu\text{-dimethylfulvene})_2(\text{HCN})_2]^{2+}$ (**2a'**).

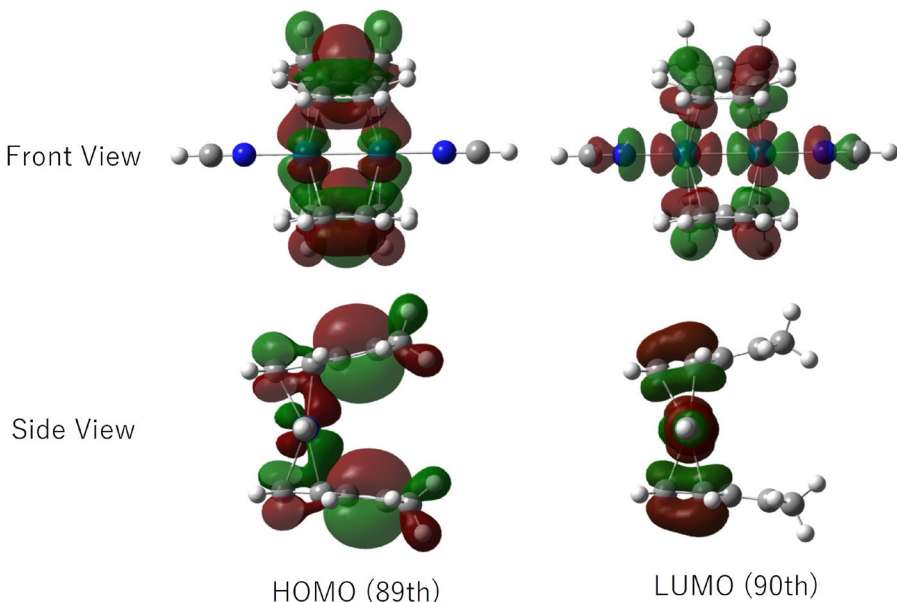


Figure S14. The selected molecular orbitals of $[\text{Pd}(\mu\text{-dimethylfulvene})_2(\text{HCN})_2]^{2+}$ (**2a'**).

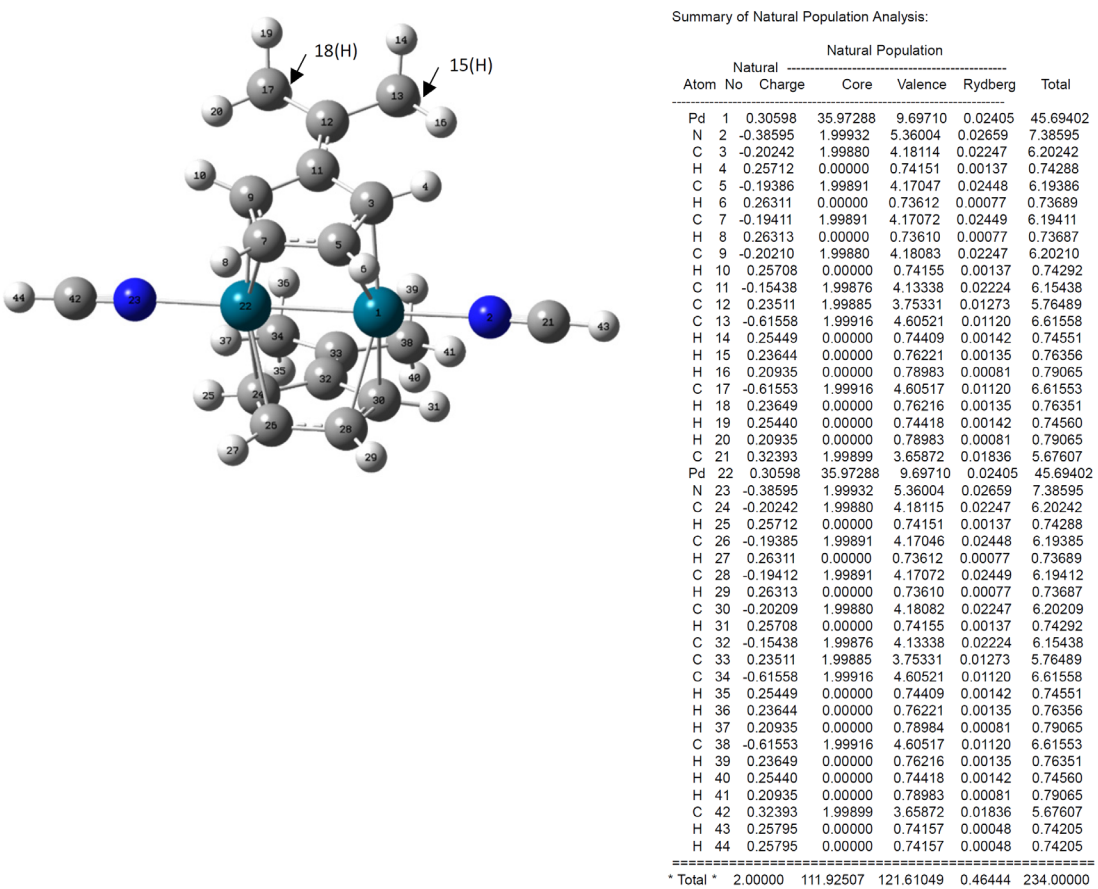


Figure S15. Summary of Natural Population Analysis of $[\text{Pd}(\mu\text{-dimethylfulvene})_2(\text{HCN})_2]^{2+}$ (**2a'**).

Table S2. Cartesian coordinates (in Å) of the optimized geometry of $[\text{Pd}_3(\mu_3\text{-dimethylfulvene})_2(\text{HCN})_2]^{2+}$ (**3a'**).

Symbol	X	Y	Z
Pd	1.1896952	-1.2910453	0.0001932
Pd	-1.4141457	-0.0000231	-0.0000040
N	1.4578275	-3.4274161	0.0004488
N	-3.6041271	-0.0000271	-0.0000034
C	0.6806538	-1.1702249	-2.1184418
H	0.3660010	-2.1722510	-2.3914611
C	2.0115230	-0.7152811	-2.1492659
H	2.8882266	-1.3348479	-2.3016331
C	2.0114913	0.7146924	-2.1494691
H	2.8881653	1.3342526	-2.3020398
C	0.6805976	1.1695797	-2.1187691
H	0.3658875	2.1715012	-2.3921134
C	-0.2106509	-0.0003442	-2.1177862
C	-1.5955306	-0.0003893	-2.2967194
C	-2.3046593	-1.2683997	-2.6618750
H	-2.2237839	-1.4302462	-3.7463931
H	-3.3714485	-1.2100797	-2.4334614
H	-1.9011013	-2.1536482	-2.1627011
C	-2.3046877	1.2675336	-2.6621679
H	-3.3715275	1.2091295	-2.4340098
H	-2.2235369	1.4293289	-3.7466698
H	-1.9013373	2.1528499	-2.1629402
C	1.6892120	-4.5481165	0.0005349
C	-4.7499369	-0.0000735	0.0000137
Pd	1.1896443	1.2910833	-0.0001895
N	1.4576945	3.4274638	-0.0004446
C	0.6806122	1.1702447	2.1184449
H	0.3659258	2.1722596	2.3914669
C	2.0114961	0.7153438	2.1492715
H	2.8881799	1.3349386	2.3016380
C	2.0115098	-0.7146296	2.1494737
H	2.8882031	-1.3341615	2.3020482
C	0.6806309	-1.1695601	2.1187721
H	0.3659538	-2.1714928	2.3921135
C	-0.2106550	0.0003335	2.1177862
C	-1.5955360	0.0003343	2.2967123
C	-2.3047131	1.2683189	2.6618678
H	-2.2238290	1.4301777	3.7463832
H	-3.3715026	1.2099550	2.4334666
H	-1.9011966	2.1535794	2.1626813
C	-2.3046491	-1.2676136	2.6621536
H	-3.3714878	-1.2092507	2.4339812

H	-2.2235105	-1.4293999	3.7466581
H	-1.9012553	-2.1529168	2.1629377
C	1.6890427	4.5481716	-0.0005328
H	1.9106968	-5.6006223	0.0005923
H	1.9104941	5.6006843	-0.0005906
H	-5.8254020	-0.0000886	0.0000324

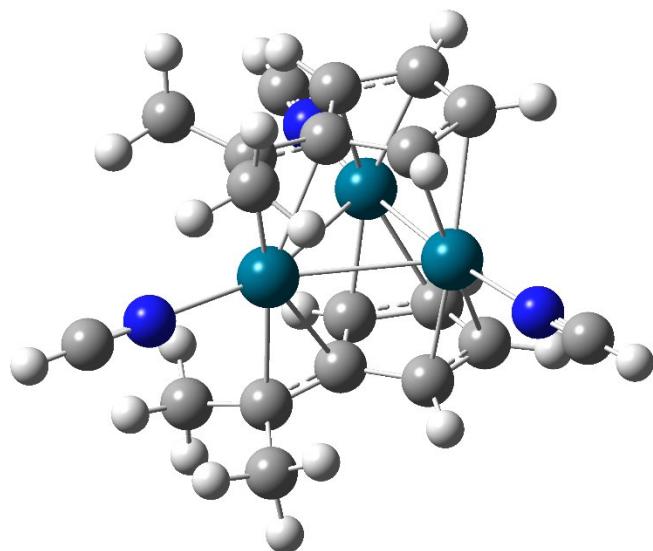


Figure S16. The optimized geometry of $[\text{Pd}_3(\mu_3\text{-dimethylfulvene})_2(\text{HCN})_2]^{2+}$ (**3a'**).

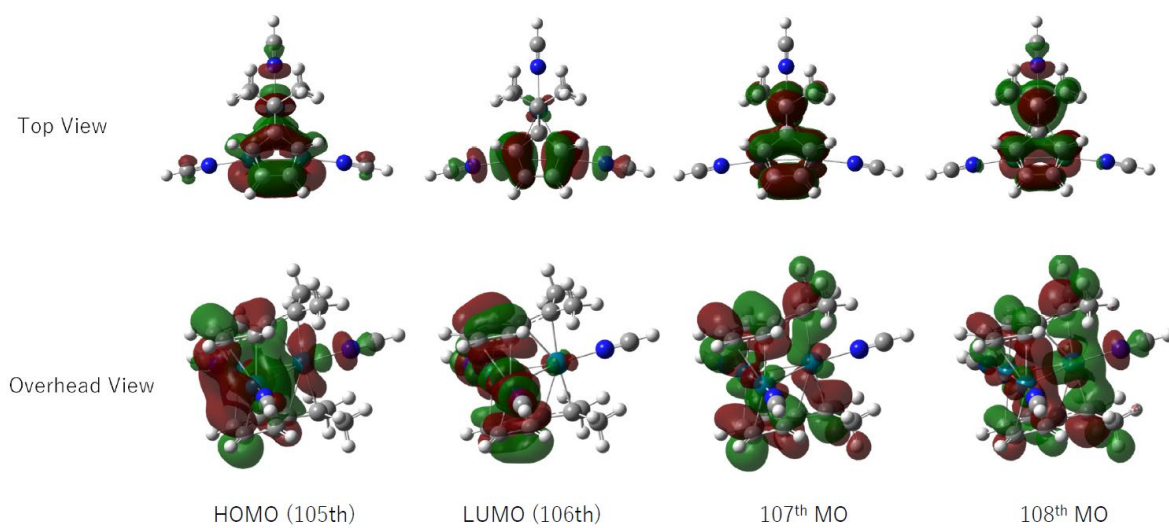


Figure S17. The selected molecular orbitals of $[\text{Pd}_3(\mu_3\text{-dimethylfulvene})_2(\text{HCN})_2]^{2+}$ (**3a'**).

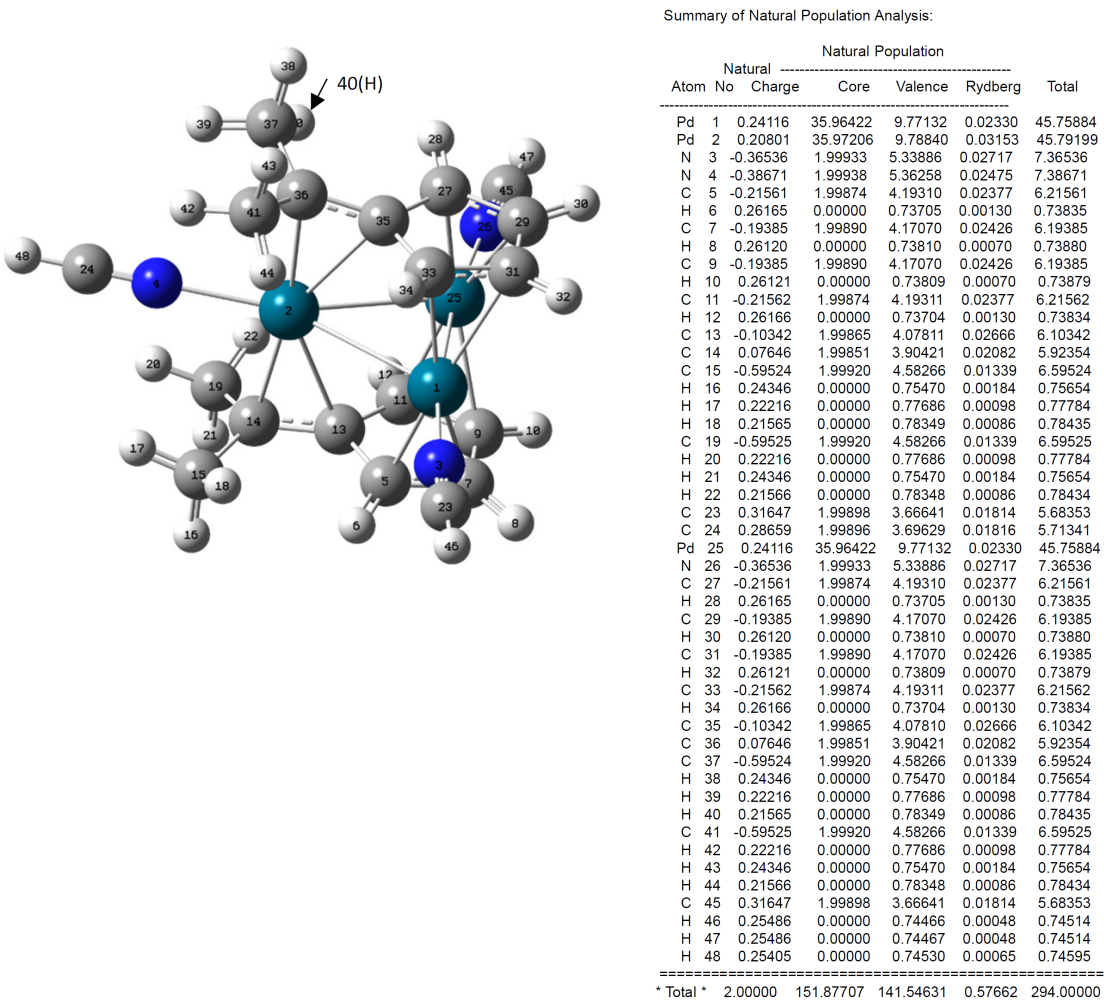


Figure S18. Summary of Natural Population Analysis of $[\text{Pd}_3(\mu_3\text{-dimethylfulvene})_2(\text{HCN})_2]^{2+}$ (**3a'**).

Table S3. Cartesian coordinates (in Å) of the optimized geometry of 6,6-dimethylfulvene.

Symbol	X	Y	Z
C	0.9657455	1.1666746	-0.0000212
H	0.6459850	2.2019359	-0.0000332
C	2.2417242	0.7290151	0.0000249
H	3.1322141	1.3495437	0.0000701
C	2.2417241	-0.7290150	0.0000149
H	3.1322139	-1.3495437	0.0000556
C	0.9657454	-1.1666745	-0.0000288
H	0.6459848	-2.2019357	-0.0000403
C	0.0821347	0.0000001	-0.0000509
C	-1.2684537	0.0000000	0.0000271
C	-2.0822427	1.2495885	0.0000090
H	-2.7437160	1.2762986	0.8768598
H	-2.7435107	1.2763612	-0.8770022
H	-1.4833792	2.1614976	0.0001073
C	-2.0822423	-1.2495886	0.0000170
H	-2.7436890	-1.2762597	-0.8768614
H	-2.7435367	-1.2764009	0.8770005
H	-1.4833783	-2.1614975	-0.0001083

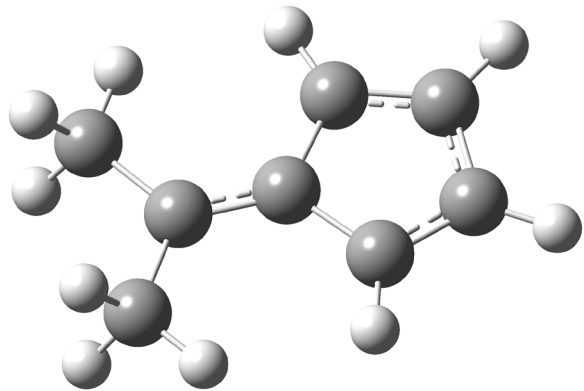


Figure S19. The optimized geometry of 6,6-dimethylfulvene.

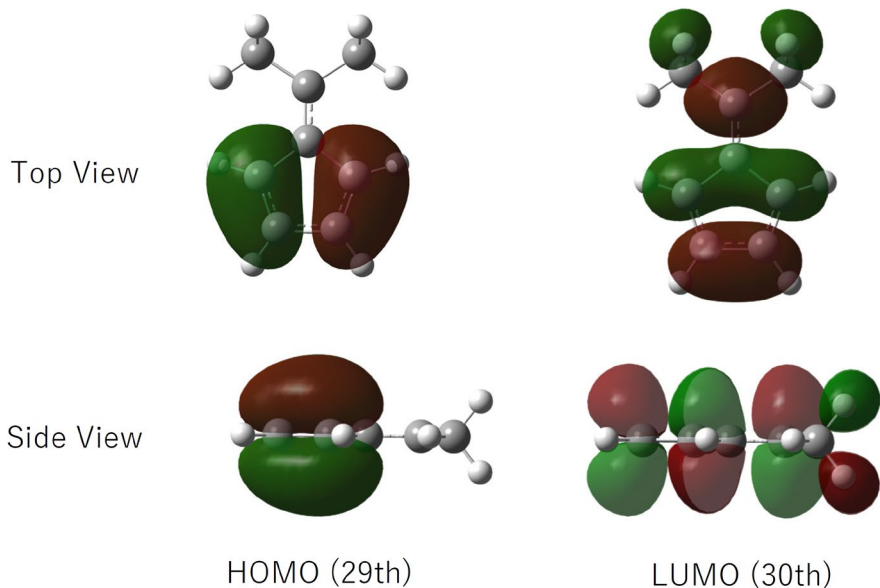


Figure S20. The selected molecular orbitals of 6,6-dimethylfulvene.

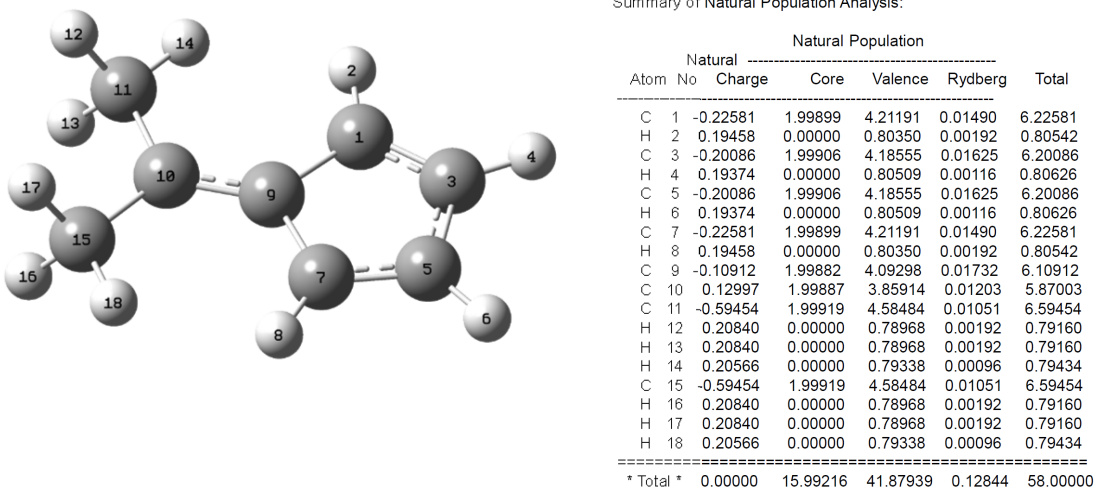


Figure S21. Summary of Natural Population Analysis of 6,6-dimethylfulvene.

Selected Bond Lengths (\AA)

Mayer Bond Index

NBO Charge

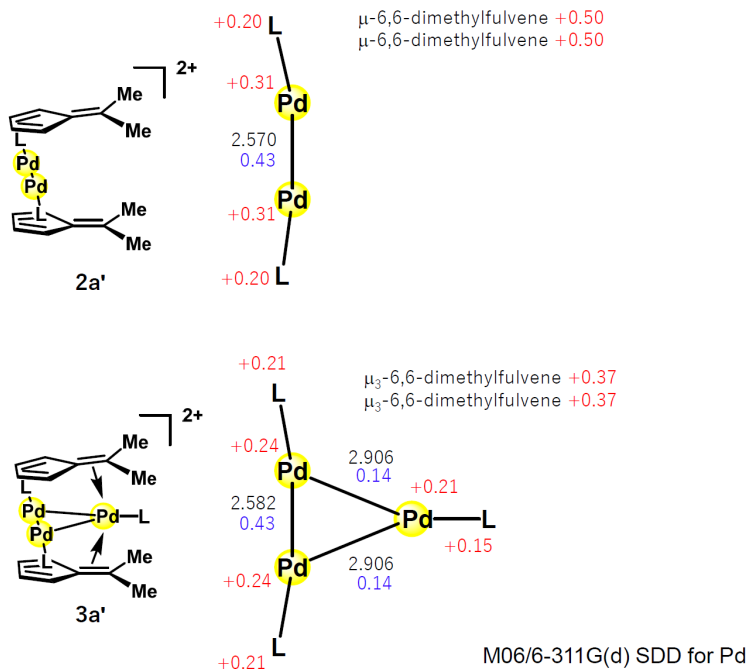


Figure S22. Summary of selected bond lengths, Mayer bond indices, and NBO charge of model complexes **2a'** and **3a'**.

X-ray Crystallographic analyses: A crystal of suitable dimensions was mounted on a CryoLoop (Hampton Research Corp.) with a layer of paraton-N oil and placed in a nitrogen stream at 123(3) K and 153(2) K. All measurements were performed on a R-AXIS RAPID imaging plate with graphite-monochromated Mo-K α (0.71075 Å) radiation. The structure was solved by direct method (SIR92,^[S9] SHELXS^[S10] or SHELXT^[S11]) and refined on F^2 by full-matrix least-squares methods; using SHELXL 2014/1, 2017/1 or 2018/3.^[S10] Non-hydrogen atoms were anisotropically refined. H-atoms were included in the refinement on calculated positions riding on their carrier atoms. The function minimized was $[\sum w(F_o^2 - F_c^2)^2]$ ($w = 1 / [\sigma^2(F_o^2) + (aP)^2 + bP]$), where $P = (\text{Max}(F_o^2, 0) + 2F_c^2) / 3$ with $\sigma^2(F_o^2)$ from counting statistics. The function $R1$ and $wR2$ were $(\sum |F_o| - |F_c|) / \sum |F_o|$ and $[\sum w(F_o^2 - F_c^2)^2 / \sum (wF_o^4)]^{1/2}$, respectively. The ORTEP-3 program was used to draw the molecule.^[S12] Crystal data for the structures reported in this paper have been deposited in the Cambridge Crystallographic Database Centre: CCDC 2211535-2211539.

X-ray Crystallographic Data

Crystal data for **2b**: $C_{42}H_{40}B_2F_8N_4O_4Pd_2$, $M_r = 1051.20$, orthorhombic, space group $Pccn$ (no. 56), $a = 31.0364(17)$ Å, $b = 14.3700(9)$ Å, $c = 19.3410(12)$ Å, $Z = 8$, $V = 8626.0(9)$ Å³, $F(000) = 4208$, $D_c = 1.619$ g cm⁻³, $\mu(\text{MoK}\alpha) = 9.15$ cm⁻¹, $T = 153$ K, 119367 reflections collected, 9874 unique ($R_{\text{int}} = 0.1636$), 560 variables refined with 4815 reflections with $I > 2\sigma(I)$ to $R = 0.0743$. CCDC 2211535.

Crystal data for **2b-Cl**: $C_{41}H_{36}Cl_6Pd_2$, $M_r = 954.20$, monoclinic, space group $C2/c$ (no. 15), $a = 29.5654(7)$ Å, $b = 12.3888(3)$ Å, $c = 23.0650(6)$ Å, $\beta = 113.2426(8)^\circ$, $Z = 8$, $V = 7762.6(3)$ Å³, $F(000) = 3808$, $D_c = 1.633$ g cm⁻³, $\mu(\text{MoK}\alpha) = 13.69$ cm⁻¹, $T = 123$ K, 83792 reflections collected, 8863 unique ($R_{\text{int}} = 0.0600$), 415 variables refined with 7462 reflections with $I > 2\sigma(I)$ to $R = 0.0325$. CCDC 2211536.

Crystal data for **3a**: $C_{29}H_{37}B_2F_8N_3Pd_3$, $M_r = 920.43$, monoclinic, space group $C2/c$ (no. 15), $a = 17.7178(7)$ Å, $b = 11.1501(5)$ Å, $c = 18.1341(8)$ Å, $\beta = 112.6707(13)^\circ$, $Z = 4$, $V = 3305.7(2)$ Å³, $F(000) = 1808$, $D_c = 1.849$ g cm⁻³, $\mu(\text{MoK}\alpha) = 16.84$ cm⁻¹, $T = 123$ K, 36990 reflections collected, 3785 unique ($R_{\text{int}} = 0.0471$), 242 variables refined with 2960 reflections with $I > 2\sigma(I)$ to $R = 0.0507$. CCDC 2211537.

Crystal data for **3b**: $C_{44.5}H_{40.5}B_2F_8N_3O_2Pd_3$, $M_r = 1142.12$, triclinic, space group $P-1$ (no. 2), $a = 13.6501(7)$ Å, $b = 13.9198(7)$ Å, $c = 14.6715(6)$ Å, $\alpha = 116.090(4)^\circ$, $\beta = 97.842(3)^\circ$, $\gamma = 110.6135(15)^\circ$, $Z = 2$, $V = 2198.2(2)$ Å³, $F(000) = 1129$, $D_c = 1.726$ g cm⁻³, $\mu(\text{MoK}\alpha) = 12.89$ cm⁻¹, $T = 153$ K, 52958 reflections collected, 10046 unique ($R_{\text{int}} = 0.1261$), 572 variables refined with 9349 reflections with $I > 2\sigma(I)$ to $R = 0.0435$. CCDC 2211538.

Crystal data for **4**: C₄₆H₄₃B₂F₈N₅Pd₃, M_r = 1158.67, monoclinic, space group *P2₁/c* (no. 14), *a* = 17.2396(6) Å, *b* = 18.0521(7) Å, *c* = 15.9775(7) Å, β = 108.5900(12)°, Z = 4, *V* = 4712.9(3) Å³, *F*(000) = 2296, *D*_c = 1.633 g cm⁻³, μ(MoKα) = 12.02 cm⁻¹, *T* = 153 K, 69046 reflections collected, 10667 unique (R_{int} = 0.0752), 554 variables refined with 7513 reflections with *I* > 2σ(*I*) to *R* = 0.0560. CCDC 2211539.

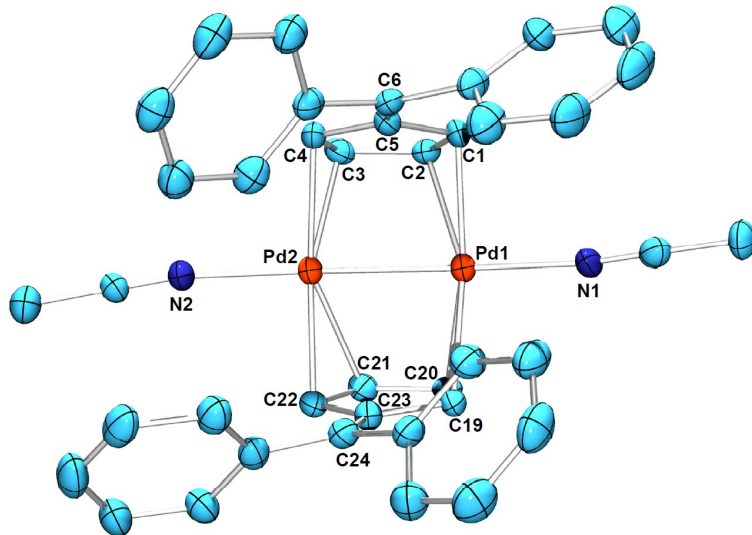


Figure S23. ORTEP of complex **2b**

Table S4. Selected Bond Distances (\AA) and Angles (deg.)

Pd1–Pd2	2.4992(8)	C1–C2	1.382(10)
Pd1–N1	2.093(7)	C2–C3	1.439(11)
Pd2–N2	2.102(6)	C3–C4	1.380(10)
Pd1–C1	2.185(7)	C4–C5	1.475(10)
Pd1–C2	2.361(7)	C5–C1	1.487(10)
Pd1–C19	2.231(7)	C5–C6	1.377(10)
Pd1–C20	2.193(6)	C19–C20	1.375(10)
Pd2–C3	2.222(7)	C20–C21	1.447(11)
Pd2–C4	2.230(7)	C21–C22	1.404(10)
Pd2–C21	2.346(7)	C22–C23	1.480(10)
Pd2–C22	2.181(7)	C23–C19	1.477(10)
		C23–C24	1.355(10)
		N1–Pd1–Pd2	169.1(2)
		N2–Pd2–Pd1	168.2(2)

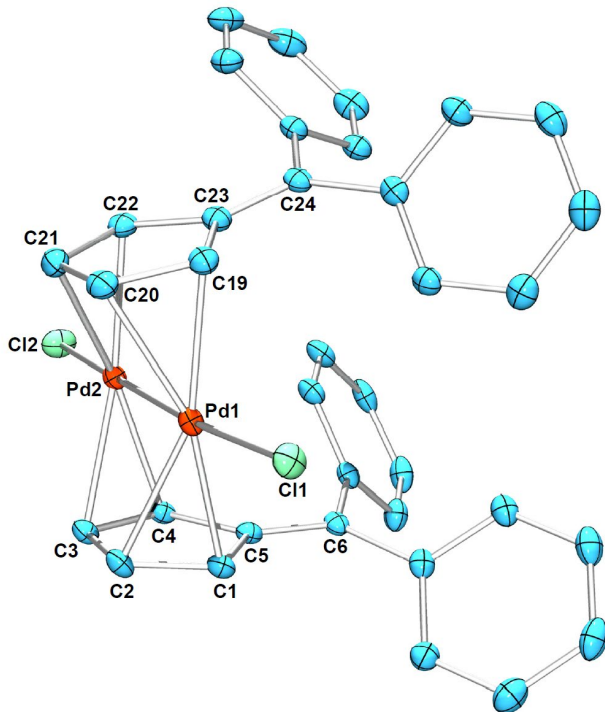


Figure S24. ORTEP of complex **2b-Cl**

Table S5. Selected Bond Distances (\AA) and Angles (deg.)

Pd1–Pd2	2.5261(3)	C1–C2	1.392(4)
Pd1–Cl1	2.3809(7)	C2–C3	1.452(4)
Pd2–Cl2	2.3883(7)	C3–C4	1.400(4)
Pd1–C1	2.198(2)	C4–C5	1.471(3)
Pd1–C2	2.309(2)	C5–C1	1.476(3)
Pd1–C19	2.202(3)	C5–C6	1.368(3)
Pd1–C20	2.237(3)	C19–C20	1.398(4)
Pd2–C3	2.247(2)	C20–C21	1.456(4)
Pd2–C4	2.188(3)	C21–C22	1.387(4)
Pd2–C21	2.273(3)	C22–C23	1.473(4)
Pd2–C22	2.221(3)	C23–C19	1.477(4)
		C23–C24	1.368(4)
		Cl1–Pd1–Pd2	173.39(2)
		Cl2–Pd2–Pd1	175.77(2)

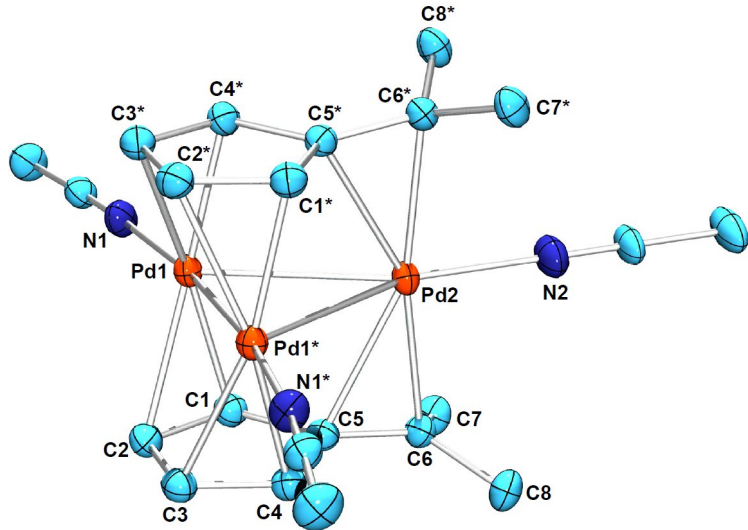


Figure S25. ORTEP of complex **3a**

Table S6. Selected Bond Distances (Å)

Pd1–Pd1*	2.5058(6)	C1–C2	1.406(7)
Pd1–Pd2	2.8694(5)	C2–C3	1.438(6)
Pd1–N1	2.096(4)	C3–C4	1.406(7)
Pd2–N2	2.087(6)	C4–C5	1.482(5)
Pd1–C1	2.156(4)	C5–C1	1.471(6)
Pd1–C2	2.314(4)	C5–C6	1.404(6)
Pd1–C3*	2.322(4)	N1–Pd1–Pd1*	172.74(11)
Pd1–C4*	2.152(4)	N2–Pd2–Pd1	154.110(8)
Pd2–C5	2.383(4)	Pd1–Pd2–Pd1*	51.780(15)
Pd2–C6	2.269(4)	Pd2–Pd1–Pd1*	64.111(8)
Pd2–C5*	2.383(4)		
Pd2–C6*	2.269(4)		

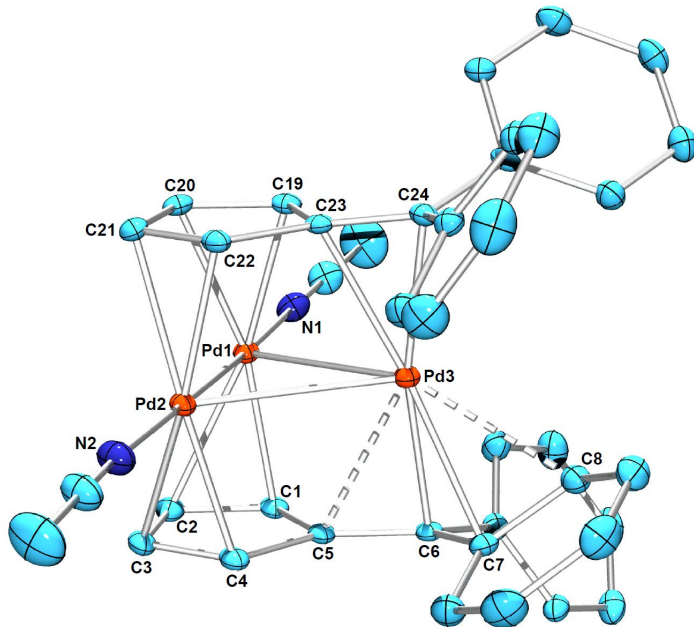


Figure S26. ORTEP of complex **3b**

Table S7. Selected Bond Distances (Å)

Pd1–Pd2	2.5010(3)	C1–C2	1.403(5)
Pd1–Pd3	2.8128(3)	C2–C3	1.444(5)
Pd2–Pd3	2.8691(3)	C3–C4	1.404(5)
Pd1–N1	2.092(3)	C4–C5	1.482(4)
Pd2–N2	2.089(3)	C5–C1	1.469(5)
Pd1–C1	2.171(3)	C5–C6	1.407(4)
Pd1–C2	2.359(3)	C6–C7	1.475(4)
Pd1–C19	2.187(3)	C19–C20	1.409(5)
Pd1–C20	2.253(3)	C20–C21	1.439(5)
Pd2–C3	2.273(3)	C21–C22	1.393(5)
Pd2–C4	2.137(3)	C22–C23	1.481(4)
Pd2–C21	2.291(3)	C23–C19	1.488(4)
Pd2–C22	2.171(3)	C23–C24	1.405(4)
Pd3–C5	2.545(3)	N1–Pd1–Pd2	177.64(9)
Pd3–C6	2.194(3)	N2–Pd2–Pd1	176.78(9)
Pd3–C7	2.354(3)	Pd1–Pd2–Pd3	62.732(9)
Pd3–C23	2.251(3)	Pd2–Pd3–Pd1	52.218(8)
Pd3–C24	2.223(3)	Pd3–Pd1–Pd2	65.050(9)

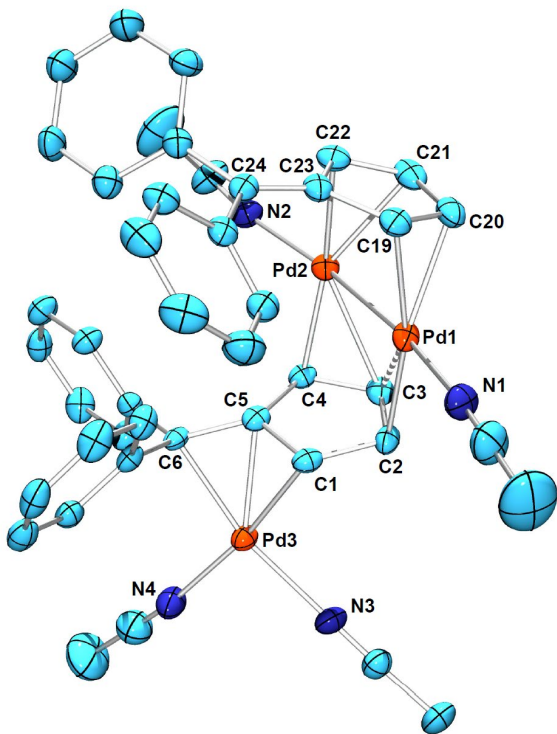


Figure S27. ORTEP of complex 4

Table S8. Selected Bond Distances (Å)

Pd1–Pd2	2.5409(6)	C1–C2	1.471(7)
Pd1–N1	2.099(5)	C2–C3	1.412(7)
Pd2–N2	2.093(5)	C3–C4	1.431(7)
Pd3–N3	2.100(5)	C4–C5	1.458(7)
Pd3–N4	2.087(5)	C5–C1	1.430(7)
Pd1–C2	2.138(5)	C5–C6	1.438(7)
Pd1–C3	2.525(5)	C19–C20	1.380(8)
Pd1–C19	2.242(5)	C20–C21	1.458(9)
Pd1–C20	2.229(5)	C21–C22	1.381(8)
Pd2–C3	2.437(5)	C22–C23	1.471(8)
Pd2–C4	2.129(5)	C23–C19	1.479(8)
Pd2–C21	2.308(5)	C23–C24	1.368(7)
Pd2–C22	2.192(5)	N1–Pd1–Pd2	172.03(15)
Pd3–C1	2.186(5)	N2–Pd2–Pd1	169.89(13)
Pd3–C5	2.154(5)		
Pd3–C6	2.142(4)		

References

- [S1] T. Murahashi, T. Nagai, T. Okuno, T. Matsutani, H. Kurosawa, *Chem. Commun.* **2000**, 1689.
- [S2] T. Ukai, H. Kawazura, Y. Ishii, J. K. Bonnet, J. A. Ibers, *J. Organomet. Chem.* **1974**, 65, 253.
- [S3] Gaussian09, Revision D.01, M. J. Frisch, G. W. Trucks, H. B. Schlegel, G. E. Scuseria, M. A. Robb, J. R. Cheeseman, G. Scalmani, V. Barone, B. Mennucci, G. A. Petersson, H. Nakatsuji, M. Caricato, X. Li, H. P. Hratchian, A. F. Izmaylov, J. Bloino, G. Zheng, J. L. Sonnenberg, M. Hada, M. Ehara, K. Toyota, R. Fukuda, J. Hasegawa, M. Ishida, T. Nakajima, Y. Honda, O. Kitao, H. Nakai, T. Vreven, J. A. Montgomery, Jr., J. E. Peralta, F. Ogliaro, M. Bearpark, J. J. Heyd, E. Brothers, K. N. Kudin, V. N. Staroverov, T. Keith, R. Kobayashi, J. Normand, K. Raghavachari, A. Rendell, J. C. Burant, S. S. Iyengar, J. Tomasi, M. Cossi, N. Rega, J. M. Millam, M. Klene, J. E. Knox, J. B. Cross, V. Bakken, C. Adamo, J. Jaramillo, R. Gomperts, R. E. Stratmann, O. Yazyev, A. J. Austin, R. Cammi, C. Pomelli, J. W. Ochterski, R. L. Martin, K. Morokuma, V. G. Zakrzewski, G. A. Voth, P. Salvador, J. J. Dannenberg, S. Dapprich, A. D. Daniels, Ö. Farkas, J. B. Foresman, J. V. Ortiz, J. Cioslowski, D. J. Fox, Gaussian, Inc., Wallingford CT, **2013**.
- [S4] Y. Zhao, D. G. Truhlar, *Theor. Chem. Acc.* **2008**, 120, 215.
- [S5] D. Andrae, U. Häußermann, M. Dolg, H. Stoll, H. Preuß, *Theor. Chim. Acta* **1990**, 77, 123.
- [S6] (a) R. Krishnan, J. S. Binkley, R. Seeger, J. A. Pople, *J. Chem. Phys.* **1980**, 72, 650. (b) A. D. McLean, G. S. Chandler, *J. Chem. Phys.* **1980**, 72, 5639.

- [S7] NBO, version 3.1, E. D. Glendening, A. E. Reed, J. E. Carpenter, F. Weinhold.
- [S8] BORDER, version 1.0, I. Mayer, Chemical Research Center, Hungarian Academy of Sciences, Budapest, **2005**.
- [S9] A. Altomare, G. Cascarano, C. Giacovazzo, A. Guagliardi, M. C. Burla, G. Polidori, M. Camalli, *J. Appl. Crystallogr.* **1994**, *27*, 435.
- [S10] (a) G. M. Sheldrick, *Acta Crystallogr.* **2008**, *A64*, 112. (b) G. M. Sheldrick, *Acta Crystallogr.* **2015**, *C71*, 3.
- [S11] G. M. Sheldrick, *Acta Crystallogr.* **2015**, *A71*, 3.
- [S12] L. J. Farrugia, *J. Appl. Crystallogr.* **2012**, *45*, 849.